Total Dose Effects and Bias Instabilities of $(NH_4)_2S$ Passivated Ge MOS Capacitors with $Hf_xZr_{1-x}O_y$ Thin Films

Yifei Mu, Yuxiao Fang, Ce Zhou Zhao, Chun Zhao, Qifeng Lu, Yanfei Qi, Ruowei Yi, Li Yang,
Ivona Z. Mitrovic, Stephen Taylor, and Paul R. Chalker

***Abstract*—The effects of biased irradiation on Ge MOS capacitors with $Hf_xZr_{1-x}O_y$ ($0.43<x<1$) gate dielectrics have been investigated. These devices were irradiated by a 662-KeV Cs^{137} γ-ray radiation source with 0.5 V or –0.5 V gate bias. Prior to irradiation exposure, leakage behavior and bias-instability of $Hf_xZr_{1-x}O_y$ films were also examined. Gate leakage current density increases with the increasing of Zr composition in gate oxide. In addition, Zr-containing dielectrics under positive bias exhibited more oxide negative trapped charges than that of HfO_2, which suggested that the oxygen-vacancy concentration in $Hf_xZr_{1-x}O_y$ was increased by the addition of Zr. Larger flat-band voltage shifts (ΔV_{FB}) were extracted under positive biased irradiation than the bias only results. The results indicate that radiation-induced interface traps (ΔN_{it}) are the dominant factor for ΔV_{FB} in HfO_2 thin films, whereas the radiation response for Zr-containing dielectrics under positive bias was mainly due to oxide traps. Under negative biased irradiation, ΔV_{FB} was attributed to the combined effect of the net oxide trapped charges and the passivation of Ge dangling bonds at the Ge/high-*k* interface. Additionally, both bias-induced and radiation-induced charge trapping have a crucial effect on radiation response of $Hf_xZr_{1-x}O_y$ at each dose level. $Hf_xZr_{1-x}O_y$ is identified as a promising gate dielectric for advanced CMOS technologies.**

***Index Terms*—Total dose effect, $Hf_xZr_{1-x}O_y$, germanium, oxide trapped charges, interface traps**

I. INTRODUCTION

As the scaling of complementary metal oxide semiconductor (CMOS) devices requires the increase in gate capacitance for better channel control, while maintaining low leakage current, high-*k* gate dielectric material has been employed to replace SiO_2 for nanoscale CMOS device applications [1-3]. Because of its relative high band gap and compatibility in contact with channel region, HfO_2 has been considered as a promising candidate for high-*k* gate dielectrics in CMOS technology [4, 5]. However, the dielectric constant of HfO_2 is not high enough to obtain the continued scaling of advanced metal oxide semiconductor field effect transistors (MOSFETs) [6]. ZrO_2 offers the benefit of a higher dielectric constant due to easier stabilization of its tetragonal phase as opposed to the monoclinic phase in crystallized HfO_2. In addition, HfO_2 and ZrO_2 are chemically similar and thus completely miscible in solid state [7, 8]. It has been reported that the addition of ZrO_2 into HfO_2 gate dielectric stabilizes the tetragonal phase and enhances the dielectric constant [9]. $Hf_xZr_{1-x}O_y$ dielectric is thus an attractive candidate for advanced gate stack applications. On the other hand, germanium (Ge) is of great interest as a promising channel material for future MOSFETs because it processes higher intrinsic carrier mobility (four times for hole and two times for electron mobility) compared with that of silicon (Si). Likewise, Ge applications can offer high compatibility with conventional Si integration technologies [10, 11]. However, a fundamental issue of the application of Ge in CMOS technology is that Ge easily forms unstable oxides GeO_x on the surfaces, which can result in a poor quality interface between the Ge channel and high-*k* dielectrics and low carrier mobility in the channel. This technological issue has been overcome by the passivation of Ge surface, which can prevent oxidation formation during device processing [12-14]. It has been reported that sulfur passivation of germanium is very effective in preventing the formation of the GeO_x at the interface, which can lead to superior Ge gate stack [15, 16]. The reduction of interface defects is attributed to the formation of Ge-S bonds and GeS species at the Ge/high-*k* surface. The electrical characteristics of Ge MOS devices with $Hf_xZr_{1-x}O_y$ gate dielectric have been investigated in recent studies [6]. It has been reported that the interface trap density and sub-threshold swing of Ge MOSFETs are clearly improved by the addition of ZrO_2 into HfO_2 gate dielectric. Therefore, Ge devices with $Hf_xZr_{1-x}O_y$ gates could be promising candidates for advanced CMOS technologies and integrated circuits.

Advanced MOS devices employed in space applications are subjected to radiation exposure which can lead to device degradation and circuit failures. Several studies suggest that, unlike conventional Si/SiO_2 case, a significant density of trapped charges can be observed in high-*k* dielectrics under long-term radiation and bias conditions [17-21]. Qualification

This paragraph of the first footnote will contain the date on which you submitted your paper for review. This research was funded in part by the National Natural and Science Foundation of China under the grant no. 11375146 and the platform promotion for Suzhou Municipal Key Lab "New Energy Techniques"

Yifei Mu, Qifeng Lu, Yuxiao Fang, Ivona Z. Mitrovic, and Stephen Taylor are with the Department of Electrical Engineering and Electronics, University of Liverpool, Liverpool L69 3GJ, UK.

Ce Zhou Zhao, Chun Zhao, and Yanfei Qi are with the Department of Electrical and Electronic Engineering, Xi'an Jiaotong-Liverpool University, Suzhou 215123, China (cezhou.zhao@xjtlu.edu.cn).

Ruowei Yi is with the Department of Chemistry, University of Liverpool, Liverpool L69 7ZD, UK.

Li Yang is with the Department of Chemistry, Xi'an Jiaotong-Liverpool University, Suzhou 215123, China

Paul R. Chalker is with the Center for Materials and Structures, School of Engineering, University of Liverpool, Liverpool L69 3GH, UK.

of high-*k* dielectrics for space applications needs far more studies to evaluate charge trapping behavior and reliability performance. Consequently, it is important to characterize the radiation response of Ge MOS devices with $Hf_xZr_{1-x}O_y$. However, very little research has been done on the total dose effects of these devices. In this work, we have investigated the total ionizing dose radiation effect on $Hf_xZr_{1-x}O_y$ thin films prepared by atomic layer deposition (ALD) deposited on $(NH_4)_2S$ passivated Ge substrate. The measurements were carried out under continuous gamma-ray exposure with positive and negative bias. The bias instability of the $Hf_xZr_{1-x}O_y$ gate dielectric with various ZrO_2 content are also studied.

II. EXPERIMENTAL DETAILS

The samples used in this study were n-type germanium (1 0 0) wafers with a doping concentration of ~10^{15} cm^{-3}. Prior to gate stack fabrication, germanium wafers were initially degreased by ultrasonic bath in acetone for 10 minutes, and then the degreased samples were ultrasonic cleaned in isopropyl alcohol for 10 minutes to remove grease or oil [15, 16]. The native oxides were then removed using a solution of HF: deionized water (1:50) for 30 seconds. The finally treatment involved a 15 minute $(NH_4)_2S$ solution (0.1 mol/L) soak and deionized water rinse in order to passivate the Ge interface [15, 16]. $Hf_xZr_{1-x}O_y$ thin films with various Zr/Hf ratio, were prepared at a wafer temperature of 200 ºC by using ALD. $Hf[(CH_3)_2N]_4$, $Zr[(CH_3)_2N]_4$, and deionized water served as the Hf precursor, Zr precursor and oxygen source. Composition and thickness of the thin films were controlled by the various ratios of Zr:Hf precursor cycles. Aluminum electrodes were deposited by electron beam evaporation with 0.07 mm^2 gate area. The physical thicknesses of HfO_2, $Hf_{0.6}Zr_{0.4}O_2$, and $Hf_{0.43}Zr_{0.57}O_2$ were 20.5 nm, 21.3 nm, and 21.1 nm respectively, as measured by spectroscopic ellipsometry. The elemental analyses of the deposited films were measured using an Oxford Instruments Energy Dispersive Spectrometer (EDS).

To investigate their radiation response, devices were irradiated at an on-site radiation response probe station system with a 662-KeV Cs^{137} γ-ray radiation source [22]. After taking into account the dose enhancement effect, the dose rate of HfO_2 and $Hf_xZr_{1-x}O_y$ thin films was 0.119 × 10^{-3} krad/s (SiO_2). A total dose up to 45 krad (SiO_2) was applied to devices with a constant gate bias of 0.5 V or -0.5 V. During the biased irradiation, oxide and interface charge trapping behaviors of $Hf_xZr_{1-x}O_y$ thin films were revealed by analysis of Capacitance-Voltage (C-V) curves at the frequency of 1 MHz. The C-V and Current-Voltage (I-V) measurements were carried out using a HP 4284 Precision LCR meter and an Agilent B1500A Semiconductor Device Analyzer.

III. RESULTS AND DISCUSSIONS

3.1 Pre-radiation and Pre-bias Characteristics

The atomic ratios of the $Hf_xZr_{1-x}O_y$ thin films investigated are shown in Table. I. Sample A was grown with the Hf:Zr deposition ratio of 1:1, (i.e. every HfO_2-H_2O cycle followed by a ZrO_2 -H_2O cycle), while the deposition ratio for sample B was 3:1. It can be observed that the atomic ratios of the thin films are 0.43:0.57 and 0.6:0.4 (Hf:Zr) for sample A and sample B, respectively. This indicates that the deposition rate of ZrO_2 is higher than that of HfO_2. Moreover, no measurable impurity has been observed in the deposited films.

TABLE. I. Energy Dispersive Spectrometer (EDS) measurements of $Hf_xZr_{1-x}O_y$ thin films on Ge (100) substrates. For ALD deposition sequence, A: Hf:Zr =1:1, B: Hf:Zr= 3:1.

Element	Weight %		Atomic %	
Sample	A	B	A	B
O	4.12	4.22	16.94	17.59
Ge	86.06	83.65	78.04	76.89
Zr	3.95	2.76	2.85	2.02
Hf	5.88	9.37	2.17	3.05

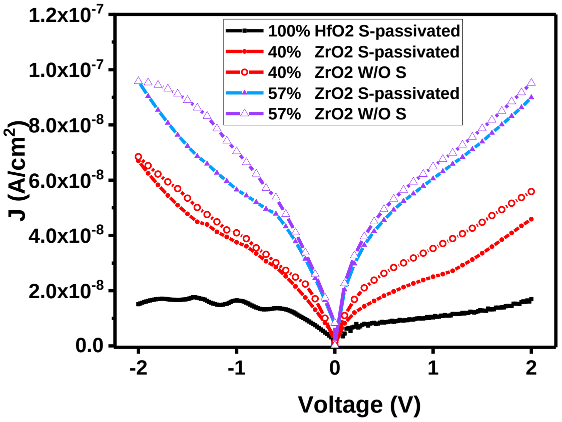

Fig. 1. Current Density-Voltage (J-V) Characteristics for $Hf_xZr_{1-x}O_y$ dielectrics on Ge MOS devices. The gate leakage density is increased with the increasing of Zr compositions in $Hf_xZr_{1-x}O_y$ gate oxide.

The impact of Zr composition in $Hf_xZr_{1-x}O_y$ gate dielectrics on their leakage behavior are exhibited in Fig. 1. It is shown that the gate leakage density is increased with the increasing of Zr composition in gate oxide. This can be explained by the smaller band gap and lower band offset of ZrO_2 compared with HfO_2. The higher leakage current density of ZrO_2 is identical to previous reports for $Hf_xZr_{1-x}O_y$ dielectric deposited on Si substrate [7]. The effects of the surface passivation of Ge on the leakage behavior in $Hf_xZr_{1-x}O_y$ MOS capacitors is also shown in Fig. 1. It can be observed that the leakage current is decreased after the sulfur treatment of Ge surface. Mao *et al.* have reported that the density and location of interface traps at dielectric/Si surface have significant effects on gate leakage current [23]. It was also reported that the passivation of Ge surface can result in the formation of high-*k*/S/Ge stack , thus decreasing the interface traps [15]. Therefore, the improved leakage characteristics in sulfur passivated samples can be attributed to the reduction of interface trap density. However, the leakage behavior of the MOS capacitors cannot fully identify the impact of sulfur treatment and Zr composition on Ge interface states. It is necessary to investigate the interface defects by evaluating bias instability of the MOS capacitors via their C-V

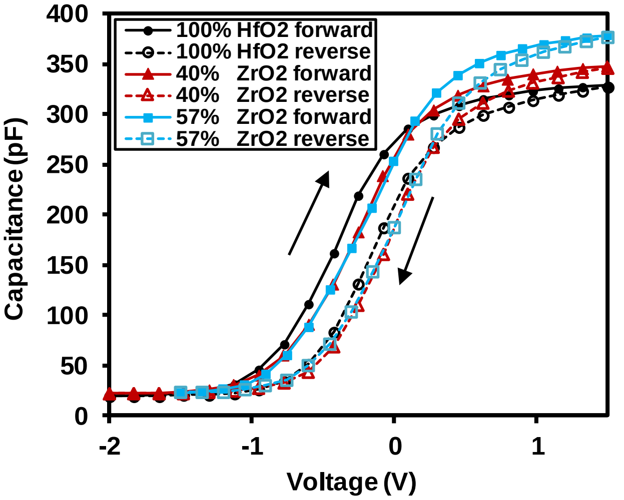

Fig. 2. Capacitance-Voltage (C-V) characteristics of Ge MOS capacitors with HfO_2, $Hf_{0.6}Zr_{0.4}O_2$, and $Hf_{0.43}Zr_{0.57}O_2$ gate dielectrics. The permittivity of gate oxide increase with the increasing of ZrO_2 compositions in $Hf_xZr_{1-x}O_y$ dielectrics.

characteristics.

Fig. 2 shows the C-V characteristics of Ge MOS capacitors with various Zr-compositions of $Hf_xZr_{1-x}O_y$ gate dielectrics. The result indicates that higher dielectric constants can be observed in Zr-doped $Hf_xZr_{1-x}O_y$ thin films. It can be understood that the addition of ZrO_2 into HfO_2 gate oxide stabilizes the tetragonal phase and shows higher dielectric constant, whereas the HfO_2 exhibits monoclinic phase as opposite to ZrO_2 [7, 8]. Smaller hysteresis was extracted from the C-V curves of MOS capacitors with $Hf_{0.43}Zr_{0.57}O_2$ and $Hf_{0.6}Zr_{0.4}O_2$ dielectrics. The hysteresis between the ramped up and ramped down of C-V curves was originated from part of the defects in high-*k* dielectrics which can be repeatedly neutralized and recharged by charge injection from the substrate [24, 25]. Therefore, the results imply that Zr-containing HfO_2 gate dielectrics has fewer cyclic charged traps or border traps compared with HfO_2. In addition, the gate ZrO_2 doped dielectrics shows a positive flat-band voltage shift (ΔV_{FB}) compared with HfO_2, which may be attributable to the presence of pre-existing electron traps or the lack of positive charges in ZrO_2.

3.2 Bias Instability

As discussed in our earlier work, the ΔV_{FB} of irradiated devices under electric field is attributed to the combined effect of radiation-induced and bias-induced charge trapping in dielectrics [26]. In order to separate the bias-instability and radiation-caused shifts, the ΔV_{FB} of the devices under electric field without radiation exposure was observed [19, 27, 28]. Fig. 3 illustrates the ΔV_{FB} of Ge MOS capacitors with various Zr-containing $Hf_xZr_{1-x}O_y$ gate dielectrics. The ΔV_{FB} were estimated by C-V measurements under -0.5 V or 0.5 V without irradiation (W/O). The inset of Fig. 3 illustrates representative CV curves of $Hf_{0.6}Zr_{0.4}O_2$ before and after different bias conditions. Under positive bias (PB), $Hf_xZr_{1-x}O_y$ with various Zr compositions all exhibited positive ΔV_{FB} up to 0.38 V. As the ΔV_{FB} was attributed to the combined effect of net oxide trapped charges and interface traps at the Ge/high-*k* interface, this positive ΔV_{FB} of $Hf_xZr_{1-x}O_y$ gate dielectrics was induced by electron tunneling from the Ge substrate to form negatively charged states and/or the build-up of interface traps. In addition, the ΔV_{FB} of the capacitors increases with the increase of Zr composition in $Hf_xZr_{1-x}O_y$. This result indicates that HfO_2 dielectrics exhibits relative low electron trap density or interface trap density compared with that of ZrO_2. Negative bias (NB) applied on the $Hf_xZr_{1-x}O_y$ capacitors for more than 130 hours without irradiation resulted in negative ΔV_{FB} up to -0.18 V. No significant discrepancy of ΔV_{FB} was observed for $Hf_xZr_{1-x}O_y$ thin films with various Zr compositions. This can be explained by an approximately equal density of both net positive oxide trapped charges and interface charges for HfO_2 and ZrO_2. However, as shown in the following results (Fig. 4), it seems more probable that the combined effect of oxide and interface charge trapping is the dominant cause for the identical ΔV_{FB} obtained under NB.

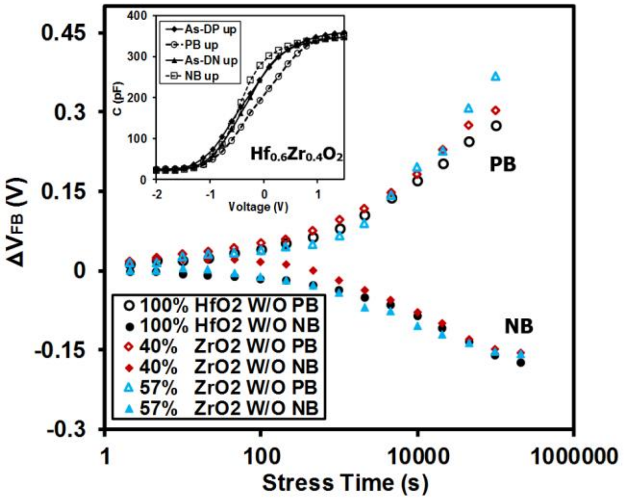

Fig. 3. Flat-band voltage shifts (ΔV_{FB}) induced by -0.5 V or 0.5 V bias without irradiation as a function of stress time for Ge MOS capacitors with $Hf_xZr_{1-x}O_y$ gate dielectrics. Under positive bias (PB), larger ΔV_{FB} were obtained from Zr-containing devices after a stress time of 130 hours. Under negative bias (NB), no significant discrepancy of ΔV_{FB} can be observed. The C-V plots of the Ge MOS capacitors with $Hf_{0.6}Zr_{0.4}O_2$ before and after pure bias without irradiation are shown in the inset.

In order to determine the charge trapping behavior in $Hf_xZr_{1-x}O_y$ gate dielectrics under pure bias conditions, oxide trap density (ΔN_{ot}) and interface trap density (ΔN_{it}) was calculated from the C-V curves used in the extraction of ΔV_{FB} in Fig. 3. J. A. Felix *et. al* reported that the mid-gap voltage shift (ΔV_{mg}) of MOS capacitors is mainly affected by the oxide trapped charges in dielectrics during the irradiation exposure [15, 16]. In other words, the variations of net oxide trapped charge density (ΔN_{ot}) of $Hf_xZr_{1-x}O_y$ in this study can be calculated from the ΔV_{mg} of Ge MOS capacitors. Using the value of ΔV_{mg}, the ΔN_{ot} can be estimated by equation (5) [15]

$$\Delta N_{ot} = -\frac{C_{ox}\Delta V_{mg}}{qA}, \qquad (5)$$

where ΔV_{mg} is the mid-gap voltage shifts obtained from C-V curves, C_{ox} is the gate capacitance of MOS capacitors, -q is the electronic charge, and A is the electrode area. The gate capacitance of MOS capacitors was obtained from C-V measurement. The electronic charge is fixed and the electrode area is determined by the evaporation processes before the irradiation exposure. Therefore, the ΔN_{ot} can be calculated by the variations of mid-gap voltage.

Similarly, it was also reported that flat-band voltage shift (ΔV_{FB}) was determined by the combined effect of oxide the effects of interface trapped charges on ΔV_{FB}, the effects trapped charges and interface trapped charges. To evaluate from oxide trapped charges need to be removed. As reported in the literature, the interface trap densities can be calculated from midgap-to-flatband stretchout of C-V curves by equation (6) [15] [26]

$$\Delta N_{it} = \frac{C_{ox}(\Delta V_{FB} - \Delta V_{mg})}{qA}, \qquad (6)$$

where ΔV_{FB} is the flat-band voltage shift obtained from C-V curves, ΔV_{mg} is the mid-gap voltage shifts obtained from C-V curves, C_{ox} is the gate capacitance of MOS capacitors, and -q is the electronic charge, and A is the electrode area. Therefore, the ΔN_{it} can be calculated by the variations of ΔV_{mg} and ΔV_{FB}.

Fig. 4 (a) shows the ΔN_{ot} as a function of stress time for both positive bias (PB) and negative bias (NB). The result indicates that the density of negative oxide trapped charges increases in magnitude with increasing Zr composition in $Hf_xZr_{1-x}O_y$ during PB. Under PB, electrons are injected from Ge substrate, the electron traps near the interface can trap the tunneling electrons and forming negative oxide trapped charges. These negative oxide trapped charges near the Ge/dielectric interface would have significant effect on mid-gap voltage and ΔN_{ot}. Therefore, the higher ΔN_{ot} of ZrO_2 indicates that the negative oxide trap density in ZrO_2 is higher than that of HfO_2. It was also reported that the possible oxide trap centers in HfO_2 and ZrO_2 are related to oxygen vacancies and interstitials (O^0/O^-) [29]. Since the oxygen vacancies in high-*k* dielectrics behave as negative oxide traps, the larger ΔN_{ot} of Zr-containing dielectrics under PB can be attributed to the higher density of oxygen vacancies in ZrO_2.

With regard to NB, ΔN_{ot} of HfO_2 was larger than that of Zr-containing $Hf_xZr_{1-x}O_y$. The result indicates that the density of positive oxide trapped charges decrease with increasing Zr composition in $Hf_xZr_{1-x}O_y$ during PB. Under PB, holes are injected from Ge substrate, the pre-existing hole traps near the interface can trap the tunneling holes and forming positive oxide trapped charges. The result indicates that more pre-existing hole traps are located in HfO_2 compared with ZrO_2. In summary, larger ΔN_{ot} for Zr-containing dielectrics under NB is attributed to the higher density of oxygen vacancies in ZrO_2, while higher ΔN_{ot} for HfO_2 under PB can be attribute to the larger density of pre-existing hole traps in HfO_2.

Fig. 4 (b) shows the ΔN_{it} for Ge MOS capacitors with $Hf_xZr_{1-x}O_y$ gate dielectrics under PB and NB. The interface trap density of $Hf_xZr_{1-x}O_y$ with various Zr compositions was all increased during PB. This can be attributed to the build-up of Ge dangling bonds at Ge/dielectrics interface. It has been reported that the passivation of Ge surface by sulfide can result in Ge-S bonds

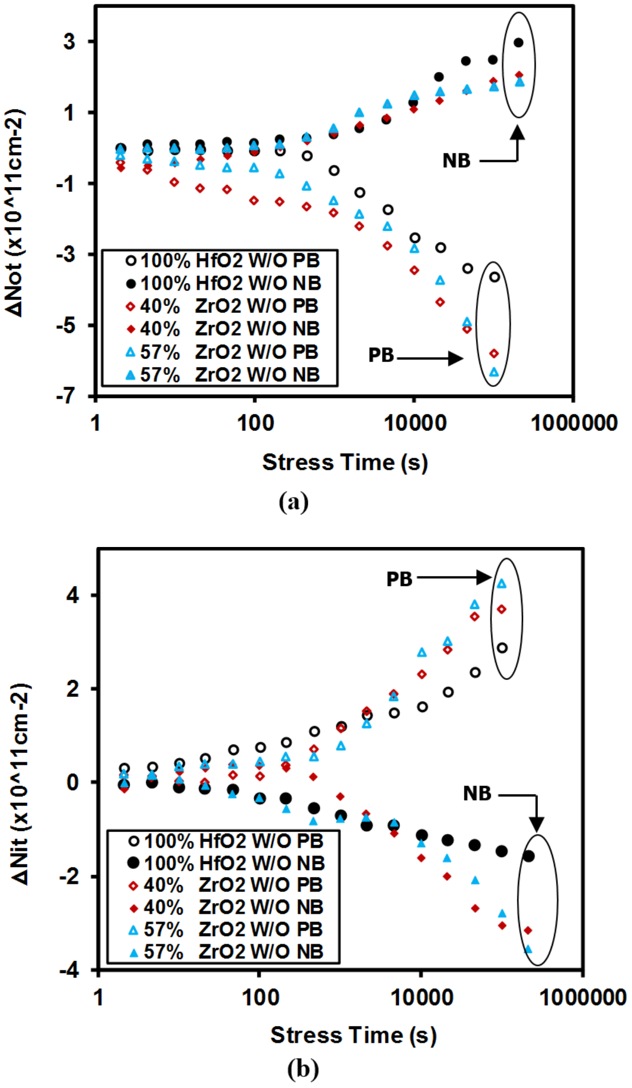

Fig. 4. (a) ΔN_{ot} and (b) ΔN_{it} as a function of stress time for Ge MOS capacitors with HfO_2, $Hf_{0.6}Zr_{0.4}O_2$, and $Hf_{0.43}Zr_{0.57}O_2$ gate dielectrics under -0.5 V or 0.5 V bias without irradiation exposure. ΔN_{ot} was extracted from the mid-gap voltage shift of C-V curves of Ge devices. ΔN_{it} was calculated from ΔV_{FB} and mid-gap voltage shift of Ge devices.

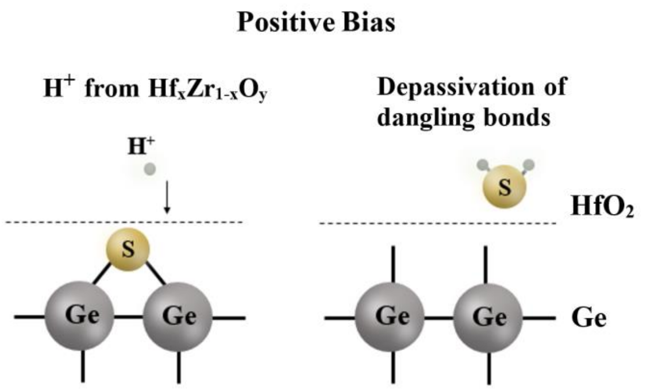

Fig. 5. The schematic diagram of Ge MOS capacitors with $Hf_xZr_{1-x}O_y$ dielectrics showing de-passivation process of Ge-S bonds. Under positive bias, H^+ ions can be generated at the anode and drift to the Ge interface to break the passivated Ge-S bonds [28, 32].

TABLE. II. Calculate N_{it} of $Hf_xZr_{1-x}O_y$ thin films at -1.8V.

Material	N_{it} at -1.8V (cm^{-2})
57% $Hf_{0.43}Zr_{0.57}O_2$ S-passivated	2.15×10^{13}
40% $Hf_{0.6}Zr_{0.4}O_2$ S-passivated	2.21×10^{13}

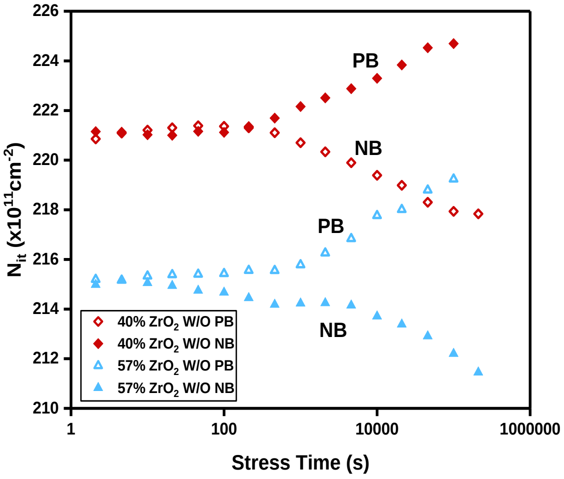

Fig. 6. N_{it} as function of stress time for $Hf_xZr_{1-x}O_y$ S-passivated thin films under -0.5V or 0.5V bias without irradiation.

and thus decrease the interface traps [12, 16]. Moreover, it is suggested that H^+ protons generated at the anode by positive bias can drift to the Ge interface and break the passivated Ge-S bonds as shown in Fig. 5 [12, 27, 30]. One possible reaction of the formation of an interface trap is shown in (7),

$$Ge - S + 2\,H^+ \rightarrow Ge^+ + H_2S \qquad (7)$$

therefore, the depassivation of passivated Ge-S bonds under positive bias can lead to an increase in interface trap density for Ge MOS capacitors. In addition, more interface traps were generated in Zr-doped $Hf_xZr_{1-x}O_y$ compared to HfO_2. The larger ΔN_{it} of Zr containing $Hf_xZr_{1-x}O_y$ suggested that ZrO_2 tended to present more hydrogen-related species than HfO_2. With regard to NB, ΔN_{it} of $Hf_xZr_{1-x}O_y$ with various Zr compositions are also increases in magnitude, but has a negative sign. In this case, Ge dangling bonds at the interface were passivated. Moreover, it can be observed that more passivated dangling bonds are generated in Zr-doped $Hf_xZr_{1-x}O_y$. However, the source for passivation and related mechanisms are not fully understood yet. The difference of ΔN_{it} between the different devices suggested that the source for passivation of dangling bonds was likely from the oxide, but not hydrogen in Ge.

Interface trap density (N_{it}) of the pristine oxides is calculated by the conductance method proposed by Nicollian and Goetzberger in 1967 [31]. The technique is based on measuring the equivalent parallel conductance G_p of an MOS capacitor as a function of bias voltage and frequency. The conductance, representing the loss mechanism due to interface trap capture

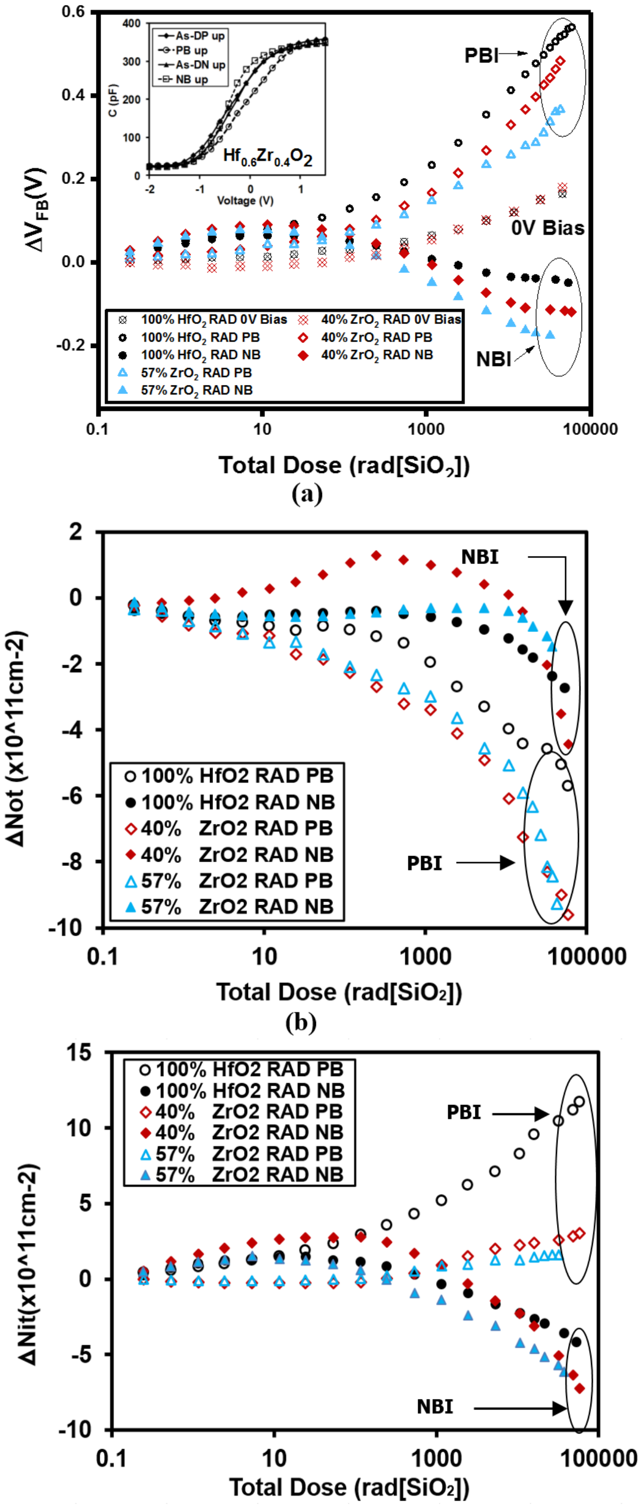

(a)

(b)

(c)

Fig. 7. (a) ΔV_{FB}, (b) ΔN_{ot}, and (c) ΔN_{it} as a function of total dose for Ge MOS capacitors with $Hf_xZr_{1-x}O_y$ gate dielectrics under -0.5 V or 0.5 V biased irradiation. The inset of (a) shows C-V plots of the Ge MOS capacitors with $Hf_{0.6}Zr_{0.4}O_2$ before and after biased irradiation. ΔV_{FB} and ΔN_{ot} were extracted from the flat-band and mid-gap voltage shift of C-V curves, respectively. ΔN_{it} was calculated from the ΔV_{FB} and mid-gap voltage shift of irradiated Ge devices.

and emission of carriers, is a measure of the interface trap density.

Capacitance-Voltage (C-V) curves were measured first to determine the mid-gap voltage and oxide capacitance (C_{ox}). Then the conductance-frequency (G_m-f) curves and capacitance-frequency (C_m-f) curves of $Hf_xZr_{1-x}O_y$ thin films were measured at determined mid-gap voltage. The frequency range was from 15 kHz to 1 MHz. All curves were measured using a HP 4284 Precision LCR meter. The $\frac{G_p}{\omega}$ was calculated by equation (3) [32]

$$\frac{G_p}{\omega} = \frac{\omega G_m C_{ox}^2}{G_m^2 + \omega^2 (C_{ox} - C_m)^2}\,, \qquad (3)$$

where $\omega = 2\pi f$, G_m is the measured conductance, C_{ox} is the oxide capacitance, C_m is the measured capacitance. Then an approximate expression giving the interface trap density in terms of the measured maximum conductance is given by equation (4) [31]

$$N_{it} \approx \frac{2.5}{q}\left(\frac{G_p}{\omega}\right)_{max}\,, \qquad (4)$$

where N_{it} is the interface trap density of the pristine oxides. The calculated N_{it} are listed in Table. II.

Table. II indicates that the interface trap density increases with the increasing of Zr composition in gate oxide. The result has a good agreement with the discussion of leakage behavior, the improved leakage characteristics in sulfur passivated and Zr contained samples can be attributed to the reduction of interface trap density. In order to further identify the variation of N_{it}, the N_{it} as a function of stress time for $Hf_xZr_{1-x}O_y$ S-passivated thin films under -0.5V or 0.5V electric field without radiation were shown in Fig. 6. Similar to the result obtained in Fig 4 (b), the N_{it} of $Hf_xZr_{1-x}O_y$ with various Zr compositions was all increased during PB, while the N_{it} of the $Hf_xZr_{1-x}O_y$ MOS capacitor was all increased in magnitude during NB.

3.3 Biased Irradiation Response

A total dose up to 45 krad (SiO_2) was applied to devices with a constant gate bias of 0.5 V or -0.5 V. This study has been focused only on the relative low-dose-rate radiation response of Ge MOS capacitors with $Hf_xZr_{1-x}O_y$. That is because the advanced microelectronics devices and circuits used in aerospace engineering are unavoidably exposed to space-like radiation, which has a relatively low radiation dose rate at 10^{-5}-10^{-9} krad (SiO_2)/s. Therefore, the dose absorption rate for dielectrics in this study is 0.119×10^{-3} krad/s (SiO_2). However, if a total dose of 1 Mrad (SiO_2) is applied to $Hf_xZr_{1-x}O_y$ thin films under the present radiation source, more than 90 days gamma-ray radiation exposure needs to be performed at this stage. Some uncertain risks are able to have significant effects to the on-site measurements system during the relative long-term test, such as probe shifts, uncertain temperature and humidity. The stress voltage and the sweeping voltage were alternately applied to the MOS device during the biased irradiation tests. The irradiation exposure was uninterrupted during measurement. During the biased irradiation, the CV measurements were employed to investigate the charge trapping mechanism of $Hf_xZr_{1-x}O_y$ film at each total dose level. The C-V curves were measured by an on-site radiation response testing system at room temperature.

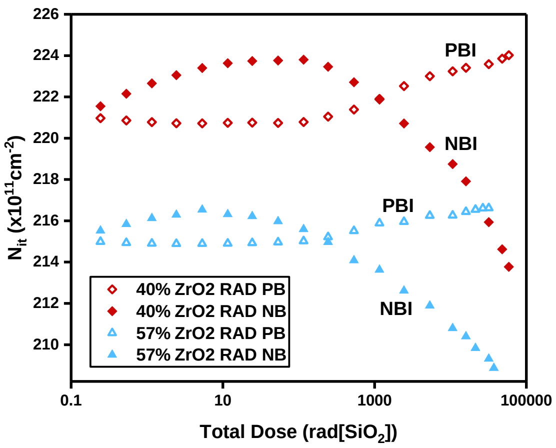

Fig. 8. N_{it} as function of total dose for $Hf_xZr_{1-x}O_y$ S-passivated thin films under -0.5V or 0.5V biased irradiation.

Fig. 7 (a) shows the ΔV_{FB} for Ge MOS capacitors with various $Hf_xZr_{1-x}O_y$ dielectrics irradiated to 45 krad (SiO_2) total dose at 0.5 V, -0.5 V and 0V. The inset of Fig. 7 (a) illustrates representative CV curves of $Hf_{0.6}Zr_{0.4}O_2$ before and after biased irradiation. Positive biased irradiation (PBI) on the devices for more than 130 hours resulted in positive ΔV_{FB} up to 0.58 V. Comparing to the result obtained from Fig. 3, larger ΔV_{FB} was extracted under radiation exposure for HfO_2 and $Hf_{0.6}Zr_{0.4}O_2$. However, the ΔV_{FB} of Ge MOS capacitors with $Hf_{0.43}Zr_{0.57}O_2$ thin films after PBI exposure is not changed significant compared to that of pure positive bias. In addition, the ΔV_{FB} of the irradiated capacitors under PBI decreased with the increasing of Zr composition in $Hf_xZr_{1-x}O_y$. On the other hand, the ΔV_{FB} of the irradiated capacitors under PBI decreased with the increasing of Zr composition in $Hf_xZr_{1-x}O_y$, which has an opposite trend compared with that of un-irradiated capacitors. Since the radiation-induced ΔV_{FB} of $Hf_xZr_{1-x}O_y$ dielectrics is determined by the density of oxide traps and interface states, the related charge trapping behavior is investigated and shown in Fig. 7 (b) and (c), respectively.

Under PBI, $Hf_xZr_{1-x}O_y$ with various Zr compositions all exhibited the presence of net negative oxide trapped charges as indicated in Fig. 7 (b). Values of these ΔN_{ot} were larger than the pure PB results in Fig. 4 (a). This enhancement was mainly caused by the net radiation-induced negative trapped charges in $Hf_xZr_{1-x}O_y$. However, the effect of oxide trapped charges to devices is more significant when the location of these charges are closer to the high-*k*/Ge interface, and the radiation-induced holes are likely to transport to high-*k*/Ge interface under positive bias [33]. The PBI exposed to $Hf_xZr_{1-x}O_y$ dielectrics is expected to induce more hole trapping. Therefore, the presence of net negative trapped charge during PBI suggests that the density of electron traps in $Hf_xZr_{1-x}O_y$ is much larger than hole traps. On the other hand, similar to the results in Fig. 4 (a), the density of negative oxide trapped charge increases with increasing Zr composition in $Hf_xZr_{1-x}O_y$. These results point to the fact that more oxygen-vacancy are located in ZrO_2 compared with HfO_2, which was observed in Fig. 4 (a).

The ΔN_{it} of the Ge MOS capacitors under PBI is shown in Fig. 7 (c). $Hf_xZr_{1-x}O_y$ with various Zr compositions all exhibited the build-up of Ge dangling bonds. Under PBI, electron-hole pairs (EHPs) can be generated and transported toward Ge substrate. During the transportation of radiation-induced holes, H^+ protons can be released from the $Hf_xZr_{1-x}O_y$ dielectrics, Hf-H, Zr-H bonds, and sub-oxide bonds [27]. As discussed in Fig. 4 (b), these H^+ protons move to the Ge interface and break the passivated Ge-S bonds, forming Ge dangling bonds. Besides, the irradiation exposure can also directly break the Hf-H, Zr-H dangling bonds, or other bonds associated with hydrogen. The ΔN_{it} of HfO_2 in Fig. 7 (c) is larger than it is observed without irradiation, whereas no significant discrepancy can be found for Zr-doped $Hf_xZr_{1-x}O_y$. The results indicated that more H^+ protons were generated in HfO_2 during PBI than that of ZrO_2, which was in contrast to the pure PB results. The results also suggested that more radiation-induced holes were generated in HfO_2, leading to higher concentration of H^+ protons during the transportation of holes. Another possible explanation is that Zr-H bond has a higher bond energy, meaning that the Zr-H bonds in ZrO_2 are less susceptible to breaking by irradiation exposure and exhibited a lower density of H^+ protons. Considering the results obtained in Figs. 7 (a)-(c), the large radiation-induced ΔN_{it} under PBI, is the predominant cause for ΔV_{FB} in Ge MOS capacitors with HfO_2. Conversely, the radiation response for Zr-containing dielectrics under positive bias is mostly affected by oxide traps. Comparing to the results evaluated in our previous study, the ΔV_{FB} evaluated in HfO_2 Ge devices is 7~8 times larger than that of Si devices, which is attributable to the large density of interface traps at the $Hf_xZr_{1-x}O_y$ / Ge interface that can result in significant effects on ΔV_{FB}.

ΔV_{FB}, ΔN_{ot}, and ΔN_{it} of the Ge MOS capacitors under negative biased irradiation (NBI) was also presented in Figs. 7 (a)-(c). After a total dose exposure up to 45 krad (SiO_2), a maximum ΔV_{FB} of -0.19 V was observed, which was comparable to the results extracted in Fig. 3. The ΔV_{FB} of the irradiated capacitors increased in terms of magnitude with the increasing of Zr composition in $Hf_xZr_{1-x}O_y$. As discussed above, this trend is likely associated with the combined effect of oxide and interface traps. In contrast to bias effects alone, the ΔN_{ot} of $Hf_xZr_{1-x}O_y$ dielectrics under NBI, indicated the presence of net negative oxide trapped charge after the total dose of 10 krad. Under NBI, the ΔN_{ot} of $Hf_{0.6}Zr_{0.4}O_2$ increases when the total dose is smaller than 1 krad and decreases when the total dose is larger than 1 krad. This trend is likely associated with the combined effect of radiation-induced negative oxide traps and bias-induced positive oxide traps under NBI.

Comparing to the result of ΔN_{ot} for $Hf_{0.6}Zr_{0.4}O_2$ extracted under pure bias in Fig. 4 (a), the results in Fig. 7 (b) indicated the presence of negative oxide trapped charges. For $Hf_{0.6}Zr_{0.4}O_2$ thin films, the accumulation of net positive charges was observed at a total dose smaller than 1 krad. However, the density of the net positive charges in Fig. 7 (b) was lower than it was observed in Fig. 4 (a). The result suggested that both bias-induced hole traps and radiation-induced electron traps dominated the oxide charge trapping of $Hf_{0.6}Zr_{0.4}O_2$ under NBI at low dose level. At a total dose larger than 10 krad, more net negative oxide trapped charges was observed in $Hf_{0.6}Zr_{0.4}O_2$ compared with lower dose. The radiation response at this dose level was mainly affected by radiation-induced negative oxide trapped charges, which can be result in the decreasing of ΔN_{ot}. The ΔN_{ot} of $Hf_xZr_{1-x}O_y$ under NBI also supported the results observed under PBI, the presence of net negative trapped charges during PBI suggested that the density of electron traps in $Hf_xZr_{1-x}O_y$ is much larger than hole traps.

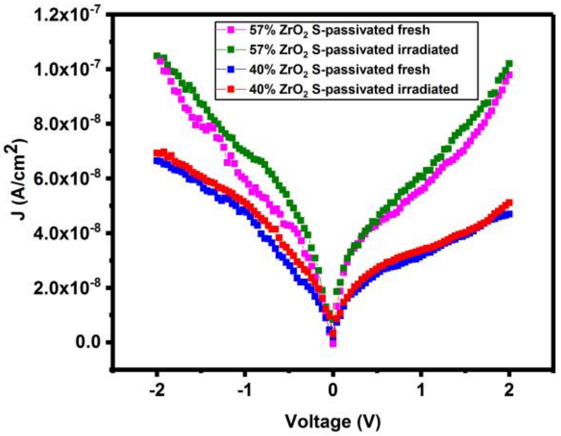

Fig. 9. Current Density-Voltage (J-V) Characteristics for $Hf_xZr_{1-x}O_y$ dielectrics on Ge MOS devices before and after irradiation exposure.

The full red markers in Fig. 7 (c) represent the ΔN_{it} of $Hf_{0.6}Zr_{0.4}O_2$ under negative bias irradiation (NBI). Under NBI, ΔN_{it} of $Hf_xZr_{1-x}O_y$ was increased in relative low dose level, while it was decrease at high does level. As discussed in section 3.2 (Bias instability), the passivation of Ge dangling bonds can lead to a decrease in interface trap density for Ge MOS capacitors, while the depassivation of passivated Ge-S bonds can lead to an increase in interface trap density for Ge MOS capacitors.

At a dose level smaller than 0.1 krad, the depassivation of passivated Ge-S bonds can be attributed to the H^+ protons drift from Ge substrate under negative bias [27]. At a total dose level larger than 0.1 krad, the passivation of Ge dangling bond dominated the interface trap density of Ge MOS capacitors. The result suggested that a large density of radiation-induced electrons are generated in oxide and transported to Ge interface to suppress the de-passivation reaction (reaction (7)) during NBI.

As discussed in Section 3.2, in order to further identify the variation of N_{it}, the N_{it} as a function of stress time for $Hf_xZr_{1-x}O_y$ S-passivated thin films under -0.5V or 0.5V biased irradiation were shown in Fig. 8. Similar to the result obtained in Fig. 7 (c), the N_{it} of $Hf_xZr_{1-x}O_y$ with various Zr compositions was all increased during PBI, while the N_{it} of the $Hf_xZr_{1-x}O_y$

MOS capacitor was all increased in magnitude during NBI.

Fig. 9 shows the I-V characteristics of MOS capacitors with $Hf_{0.43}Zr_{0.57}O_2$ and $Hf_{0.6}Zr_{0.4}O_2$ gate dielectrics before and after the irradiation exposure. The result indicates that no significant discrepancy of leakage gate current can be observed before and after the irradiation exposure for both $Hf_{0.43}Zr_{0.57}O_2$ and $Hf_{0.6}Zr_{0.4}O_2$ capacitors. The result in Fig. 9 has a good agreement with the results obtained in literature, which indicated that gate leakage current of MOS devices is insensitive to irradiation exposure. It was suggested that the radiation-induced oxide and interface trapped charges had no significant effects on leakage current. Another possible explanation is that the $Hf_xZr_{1-x}O_y$ thin films is relative thick (~20nm). The irradiation exposure has no significant effect on the leakage behavior of MOS capacitors with high-*k* dielectrics larger than 10 nm. It is reported the radiation can induce leakage current in ultra-thin gate oxides (4-7nm) [34-36]. Electrons can tunnel through the oxide and be mediated by neutral oxide defects at low oxide field, which caused radiation induced leakage current [34-36]. For the relative thick gate oxide, the radiation induced charges is difficult to tunnel the dielectric and enhance the gate leakage current.

IV. CONCLUSIONS

We have examined the radiation response of Ge MOS capacitors with $Hf_xZr_{1-x}O_y$ ($0.43<x<1$) gate dielectrics under positive and negative bias. Gate leakage current density increased with the increasing of Zr composition in gate oxide, and decreased with the sulfur treatment of Ge surface. The density of negative oxide trapped charge increases in magnitude with increasing Zr composition in $Hf_xZr_{1-x}O_y$ during PB. Under NB, ΔN_{ot} of HfO_2 was larger than that of Zr-containing $Hf_xZr_{1-x}O_y$. In addition, the difference of ΔN_{ot} between $Hf_{0.43}Zr_{0.57}O_2$ and $Hf_{0.6}Zr_{0.4}O_2$ was negligible. This implies that the concentration of oxygen vacancies and hole traps in Zr-containing $Hf_xZr_{1-x}O_y$ is not strongly dependent on Zr composition. More interface traps were generated in Zr-doped $Hf_xZr_{1-x}O_y$ compared to HfO_2 under PB, which suggests that ZrO_2 presented more hydrogen-related species than HfO_2. Under PBI, the Zr-doped $Hf_xZr_{1-x}O_y$ exhibited smaller ΔV_{FB} than that of HfO_2. This is attributed to the de-passivation of Ge-S bonds in capacitors incorporating HfO_2 thin films, resulting in the build-up of interface traps. Under NBI, ΔV_{FB} was dependent on the combined effect of the net oxide trapped charge and interface traps at the Ge/high-k interface. The ΔV_{FB} evaluated in HfO_2 Ge devices is much larger than that of the Si devices evaluated in our previous study. This can be explained by the large number of interface traps between the dielectric and the Ge substrate. This work demonstrated that $Hf_xZr_{1-x}O_y$ may be a promising candidate for space microelectronics in specified bias conditions. However, the biased radiation environment is quite challenging for Ge devices, and future work will be required to identify the radiation hardness of these devices.

ACKNOWLEDGMENT

This research was funded in part by the National Natural Science Foundation of China under the grant no. 11375146 and the platform promotion for Suzhou Municipal Key Lab "New Energy Techniques".

REFERENCE

[1] J. Robertson, "High dielectric constant gate oxides for metal oxide Si transistors," *Rep. Prog. Phys.*, vol. 69, No. 2, pp. 327-396, Feb 2006.

[2] N. Raghavan, K. L. Pey, and K. Shubhakar, "High-*k* dielectric breakdown in nanoscale logic devices - Scientific insight and technology impact," *Microel. Reliab.*, vol. 54, No. 5, pp. 847-860, May 2014.

[3] G. D. Wilk, R. M. Wallace, and J. M. Anthony, "High-*k* gate dielectrics: Current status and materials properties considerations," *J. Appl. Phys.*, vol. 89, No. 10, pp. 5243-5275, May. 2001.

[4] N. Miyata, "Study of Direct-Contact HfO_2/Si Interfaces," *Materials*, vol. 5, No. 3, pp. 512-527, Mar 2012.

[5] J. Robertson, "Band offsets, Schottky barrier heights, and their effects on electronic devices," *J. Vac. Sci. Technol. A*, vol. 31, No. 5, p. 050821, Sep 2013.

[6] C. C. Li, K. Shu, C. Liao, W. F. Chi, M. C. Li, T. C. Chen, T. H. Su, Y. W. Chang, C. C. Tsai, L. J. Liu, C. H. Fu, and C. C. Lu, "Improved Electrical Characteristics of Ge pMOSFETs With ZrO_2/HfO_2 Stack Gate Dielectric," *IEEE Electron Device Lett.*, vol. 37, No. 1, pp. 12-15, Jan. 2016.

[7] H. S. Jung, S. A. Lee, S. h. Rha, S. Y. Lee, H. K. Kim, D. H. Kim, K. H. Oh, J. M. Park, W. H. Kim, M. W. Song, N. I. Lee, and C. S. Hwang, "Impacts of Zr Composition in $Hf_{1-x}Zr_xO_y$ Gate Dielectrics on Their Crystallization Behavior and Bias-Temperature-Instability Characteristics," *IEEE Trans. Electron Devices*, vol. 58, No. 7, pp. 2094-2103, 2011.

[8] R. I. Hegde, D. H. Triyoso, S. B. Samavedam, and B. E. White, "Hafnium zirconate gate dielectric for advanced gate stack applications," *J. Appl. Phys.*, vol. 101, No. 7, p. 074113, Apr 2007.

[9] T. S. Boscke, P. Y. Hung, P. D. Kirsch, M. A. Quevedo-Lopez, and R. Ramirez-Bon, "Increasing permittivity in HfZrO thin films by surface manipulation," *Appl. Phys. Lett.*, vol. 95, No. 5, p. 052904, Aug 2009.

[10] Y. Oshima, M. Shandalov, Y. Sun, P. Pianetta, and P. C. McIntyre, "Hafnium oxide/germanium oxynitride gate stacks on germanium: Capacitance scaling and interface state density," *Appl. Phys. Lett.*, vol. 94, No. 18, p. 183102, May 2009.

[11] R. Zhang, T. Iwasaki, N. Taoka, M. Takenaka, and S. Takagi, "High-Mobility Ge pMOSFET With 1-nm Al_2O_3/GeO_x/Ge Gate Stack Fabricated by Plasma Post Oxidation," *IEEE Trans. Electron Devices*, vol. 59, No. 2, pp. 335-341, 2012.

[12] T. F. Teng, S. Nachimuthu, W. H. Hung, and J. C. Jiang, "A first principles study of H_2S adsorption and decomposition on a Ge(100) surface," *Rsc Adv.*, vol. 5, No. 5, pp. 3825-3832, 2015.

[13] S. Sioncke, J. Ceuppens, D. Lin, L. Nyns, A. Delabie, H. Struyf, S. De Gendt, M. Muller, B. Beckhoff, and M. Caymax, "Atomic layer deposition of Al_2O_3 on S-passivated Ge," *Microel. Eng.*, vol. 88, No. 7, pp. 1553-1556, Jul 2011.

[14] C. X. Li, C. D. Wang, C. H. Leung, P. T. Lai, and J. P. Xu, "A study on fluorine incorporation in Ge p-MOS capacitors with HfTiON dielectric," *Microel. Eng.*, vol. 86, No. 7-9, pp. 1596-1598, Jul-Sep 2009.

[15] M. Althobaiti, S. Mather, N. Sedghi, V. R. Dhanak, I. Z. Mitrovic, S. Hall, and P. R. Chalker, "Hafnia and alumina on sulphur passivated germanium," *Vacuum*, vol. 122, No. pp. 306-309, Dec 2015.

[16] M. Milojevic, C. L. Hinkle, F. S. Aguirre-Tostado, H. C. Kim, E. M. Vogel, J. Kim, and R. M. Wallace, "Half-cycle atomic layer deposition reaction studies of Al_2O_3 on $(NH_4)_2S$ passivated GaAs(100) surfaces," *Appl. Phys. Lett.*, vol. 93, No. 25, p. 252905, Dec 2008.

[17] D. Cao, X. H. Cheng, T. T. Jia, L. Zheng, D. W. Xu, Z. J. Wang, C. Xia, Y. H. Yu, and D. S. Shen, "Total-Dose Radiation Response of HfLaO Films Prepared by Plasma Enhanced Atomic Layer

Deposition," *IEEE Trans. Nucl. Sci.,* vol. 60, No. 2, pp. 1373-1378, Apr. 2013.

[18] N. Martinez, O. Gilard, and G. Quadri, "Total Dose Effects: A New Approach to Assess the Impact of Radiation on Device Reliability," *IEEE Trans. Nucl. Sci.,* vol. 60, No. 3, pp. 2266-2271, 2013.

[19] G. X. Duan, C. X. Zhang, E. X. Zhang, J. Hachtel, D. M. Fleetwood, R. D. Schrimpf, R. A. Reed, M. L. Alles, S. T. Pantelides, G. Bersuker, and C. D. Young, "Bias Dependence of Total Ionizing Dose Effects in SiGe-SiO_2/HfO_2 pMOS FinFETs," *IEEE Trans. Nucl. Sci.,* vol. 61, No. 6, pp. 2834-2838, Dec. 2014.

[20] D. K. Chen, R. D. Schrimpf, D. M. Fleetwood, K. F. Galloway, S. T. Pantelides, A. Dimoulas, G. Mavrou, A. Sotiropoulos, and Y. Panayiotatos, "Total dose response of Ge MOS capacitors with HfO_2/Dy_2O_3 gate stacks," *IEEE Trans. Nucl. Sci.,* vol. 54, No. 4, pp. 971-974, Aug 2007.

[21] J. A. Felix, D. M. Fleetwood, R. D. Schrimpf, J. G. Hong, G. Lucovsky, J. R. Schwank, and M. R. Shaneyfelt, "Total-dose radiation response of Hafnium-silicate capacitors," *IEEE Trans. Nucl. Sci.,* vol. 49, No. 6, pp. 3191-3196, 2002.

[22] Y. Mu, C. Z. Zhao, Y. Qi, S. Lam, C. Zhao, Q. Lu, Y. Cai, I. Z. Mitrovic, S. Taylor, and P. R. Chalker, "Real-time and on-site γ-ray radiation response testing system for semiconductor devices and its applications," *Nucl. Instr. Meth. Phys. Res. B,* vol. 372, No. pp. 14-28, Apr. 2016.

[23] L. F. Mao, "Investigating the effects of the interface defects on the gate leakage current in MOSFETs," *Appl. Surf. Sci.,* vol. 254, No. 20, pp. 6628-6632, Aug 2008.

[24] C. Z. Zhao, J. F. Zhang, M. H. Chang, A. R. Peaker, S. Hall, G. Groeseneken, L. Pantisano, S. De Gendt, and M. Heyns, "Stress-induced positive charge in Hf-based gate dielectrics: Impact on device performance and a framework for the defect," *IEEE Trans. Electron Devices,* vol. 55, No. 7, pp. 1647-1656, Jul. 2008.

[25] C. Z. Zhao, J. F. Zhang, M. B. Zahid, B. Govoreanu, G. Groeseneken, and S. De Gendt, "Determination of capture cross sections for as-grown electron traps in HfO_2/HfSiO stacks," *J. Appl. Phys.,* vol. 100, No. 9, p. 093716, Nov. 2006.

[26] Y. Mu, C. Z. Zhao, Q. Lu, C. Zhao, Y. Qi, S. Lam, I. Z. Mitrovic, S. Taylor, and P. R. Chalker, "Total Ionizing Dose Response of Hafnium-Oxide Based MOS Devices to Low-Dose-Rate Gamma Ray Radiation Observed by Pulse CV and On-Site Measurements," *IEEE Trans. Nucl. Sci.,* vol. PP, No. 99, pp. 1-1, Dec 2016.

[27] X. J. Zhou, D. M. Fleetwood, L. Tsetseris, R. D. Schrimpf, and S. T. Pantelides, "Effects of Switched-bias Annealing on Charge Trapping in HfO_2 Gate Dielectrics," *IEEE Trans. Nucl. Sci.,* vol. 53, No. 6, pp. 3636-3643, Dec. 2006.

[28] J. X. Zhang, Q. Guo, H. X. Guo, W. Lu, C. H. He, X. Wang, P. Li, and M. Liu, "Impact of Bias Conditions on Total Ionizing Dose Effects of Co-60 gamma in SiGe HBT," *IEEE Trans. Nucl. Sci.,* vol. 63, No. 2, pp. 1251-1258, Apr 2016.

[29] M. N. U. Bhuyian, S. Poddar, D. Misra, K. Tapily, R. D. Clark, S. Consiglio, C. S. Wajda, G. Nakamura, and G. J. Leusink, "Impact of cyclic plasma treatment on oxygen vacancy defects in TiN/HfZrO/SiON/Si gate stacks," *Appl. Phys. Lett.,* vol. 106, No. 19, p. 193508, May 2015.

[30] K. Onishi, C. Rino, K. Chang Seok, C. Hag-Ju, K. Young Hee, R. E. Nieh, H. Jeong, S. A. Krishnan, M. S. Akbar, and J. C. Lee, "Bias-temperature instabilities of polysilicon gate HfO_2 MOSFETs," *IEEE Trans. Electron Devices,* vol. 50, No. 6, pp. 1517-1524, 2003.

[31] E. H. Nicollian and A. Goetzberger, "The Si-SiO_2 interface—Electrical properties as determined by the metal-insulator-silicon-conductance technique," *Microel. Reliab.,* vol. 7, No. 2, pp. 1055-1133, 1968.

[32] D. K. Schroder, *Semiconductor Material and Device Characterization* vol. 6.3: John Wiley & Sons, 2006.

[33] V. A. K. Raparla, S. C. Lee, R. D. Schrimpf, D. M. Fleetwood, and K. F. Galloway, "A model of radiation effects in nitride-oxide films for power MOSFET applications," *Solid State Electron.,* vol. 47, No. 5, pp. 775-783, May. 2003.

[34] L. Larcher, A. Paccagnella, M. Ceschia, and G. Ghidini, "A Model of Radiation Induced Leakage Current (RILC) in Ultra-Thin Gate Oxides," *IEEE Trans. Nucl. Sci.,* vol. 46, No. pp. 1553-1561, 1999.

[35] M. Ceschia, A. Paccagnella, and A. Cester, "Radiation Leakage Current and Stress Induced Leakage Current in Ultra-Thin Gate Oxides," *IEEE Trans. Nucl. Sci.,* vol. 45, No. 6, pp. 2375-2382, 1998.

[36] A. Scarpa', A. Paccagnella', and F. Montera', "Ionizing Radiation Induced Leakage Current on Ultra-Thin Gate Oxides," *IEEE Trans. Nucl. Sci.,* vol. 44, No. 6, pp. 1818-1825, 1997.